Information distances for radar resolution analysis

Pribić, Radmila; Leus, Geert

Information Distances for Radar Resolution Analysis

Radmila Pribić
Sensors Advanced Developments
Thales Nederland
Delft, The Netherlands

Geert Leus
Electrical Engineering, Mathematics and Computer Science
Delft University of Technology
Delft, The Netherlands

Abstract— A stochastic approach to resolution based on information distances computed from the geometry of data models which is characterized by the Fisher information is explored. Stochastic resolution includes probability of resolution and signal-to-noise ratio (SNR). The probability of resolution is assessed from a hypothesis test by exploiting information distances in a likelihood ratio. Taking SNR into account is especially relevant in compressive sensing (CS) due to its fewer measurements. Based on this information-geometry approach, we demonstrate the stochastic resolution analysis in test cases from array processing. In addition, we also compare our stochastic resolution bounds with the actual resolution obtained numerically from sparse signal processing which nowadays is a major component of the back end of any CS sensor. Results demonstrate the suitability of the proposed stochastic resolution analysis due to its ability to include crucial features in the resolution performance guarantees: array configuration or sensor design, SNR, separation and probability of resolution.

Keywords— *resolution; information geometry; likelihood ratio; compressive sensing; array processing; radar;*

I. INTRODUCTION

Resolution is primarily described by the minimum distance between two objects that still can be resolved (e.g. [1]). Stochastic resolution has been introduced ([2]) by including the Cramér-Rao bound (CRB). This stochastic approach was extended with the probability of resolution at a given separation and signal-to-noise ratio (SNR) obtained via an asymptotic generalized likelihood ratio (GLR) test based on Euclidean distances ([3]). Information resolution has also been explored with an arbitrary test ([4]). Information geometry (IG, [5-6]) and compressive sensing (CS, [7-9]) have the potential to contribute to the completeness of the stochastic approach, due to their focus on information content ([10-14]). In [12-13], the Fisher-Rao information distance is recognized in the asymptotic GLR. In this paper, links to other types of information distances in resolution analysis are sought.

In the IG-based resolution analysis, the Fisher information matrix (FIM) is employed for computing resolution bounds. This stochastic approach is crucial when using fewer measurements which are typical for compressive data acquisition in the front end of a CS sensor (e.g. [7]). In the back-end, resolution metrics quantify the high-resolution performance of sparse signal processing (SSP). SSP can be seen as a model-based refinement of existing processing (e.g. [14]). Despite substantial CS research during the last decade (e.g. [7-9]), complete guarantees of CS resolution performance have

not been developed yet. Both IG and CS can improve data acquisition and signal processing due to their focus on the information content rather than the sensing bandwidth only.

The resolution ability is primarily given by sensor design, namely by the sensing bandwidth. In array processing, this deterministic resolution relies on the sensor wavelength and the array size. The stochastic resolution analysis includes also the SNR available from the data acquisition. This is expected, since besides the sensor design, the SNR and the separation of targets matter. In [12-13], we assess the probability of resolution at a given SNR and separation by applying the Fisher-Rao information distance in the asymptotic distribution of the GLR.

In this paper, the stochastic resolution analysis is extended with tighter resolution bounds obtained via an LR test and different types of information distances. In Section II, a typical radar application is summarized with the modeling of array measurements and the related SSP (as needed in Section III). In Section III, our stochastic resolution analysis is explained which includes information distances and (G)LR tests. In particular, parameters of the distribution of the LR are revealed as directly related to the information distances. For the sake of completeness, the resolution probability from SSP is numerically assessed and compared with the resolution bounds. The effects of fewer measurements, which are typical for a CS sensor, are also explored. In Section IV, numerical results from the stochastic resolution analysis are presented. In the end, conclusions are drawn and future work indicated.

II. ARRAY SIGNAL MODELLING AND PROCESSING

In a typical radar application, measurements from a spatial or temporal one-dimensional array are exploited for estimation of angle or Doppler information, respectively. The data models for array processing and, especially, for the related sparse signal processing (SSP) required in Section III are summarized here.

In an array of size M, the mth measurement y_m, $m = 1,2,\dots,M$, from K point-targets is given by ([15]):

$$y_m = \sum_{k=1}^{K} \alpha_k e^{j\beta_m \theta_k} + z_m = \sum_{k=1}^{K} \mu_m(\theta_k) + z_m, \quad (1)$$

where α_k is the kth-target echo, β_m is an observation variable (centered, i.e. $\sum_m \beta_m = 0$), θ_k is an unknown parameter and z_m is complex-Gaussian noise with zero mean and variance γ, $z_m \sim CN(0, \gamma)$. The target echo α is assumed to have constant nonrandom amplitude α_0, $\alpha_0 = |\alpha|$ (so-called SW0, [16]), and thus, the signal-to-noise ratio (SNR) equals α_0^2/γ. Signals from

both spatial or temporal arrays are described by the model function $\mu_m(\theta)$ in (1). In a spatial array, β_m and θ would yield the antenna-element position and unknown angle, respectively, while in a temporal array, β_m and θ would represent the sampling time and unknown Doppler, respectively.

In SSP, the data from (1) form a vector $\boldsymbol{y}$, $\boldsymbol{y} \in \mathbb{C}^M$, given by:

$$\boldsymbol{y} = \boldsymbol{A}\boldsymbol{x} + \boldsymbol{z} = \boldsymbol{\mu}(\boldsymbol{\theta}) + \boldsymbol{z} \,, \qquad (2)$$

where $\boldsymbol{A} \in \mathbb{C}^{M \times N}$ is a sensing matrix at M observations β_m and N parameters θ_n on a discrete grid $\boldsymbol{\theta}$, $n = 1, 2, ..., N$, $\boldsymbol{x} \in \mathbb{C}^N$ is a sparse target profile and $\boldsymbol{z} \in \mathbb{C}^M$ is the noise vector, $\boldsymbol{z} \sim CN(\boldsymbol{0}, \gamma \boldsymbol{I}_M)$. Multiple point-targets can be captured by this model, where the sparsity order of $\boldsymbol{x}$ is related to their number K in (1), $K < N$. SSP ([7] and [17]), $0 \leq p \leq 1$, applies as:

$$\boldsymbol{x}_{\text{SSP}} = \arg\min_{\boldsymbol{x}} \|\boldsymbol{y} - \boldsymbol{A}\boldsymbol{x}\|^2 + \eta \|\boldsymbol{x}\|_{\text{p}} \,, \qquad (3)$$

where the l_{p}-norm promotes sparsity, the l_2-norm minimizes the errors, and a parameter η regulates the two tasks. In radar, the parameter η is closely related to the detection threshold (e.g. [14] and [18]). The SSP in (3) relies on the incoherence of $\boldsymbol{A}$ and the sparsity, i.e. only K nonzeros in $\boldsymbol{x}$, $K < M \leq N$ (e.g. [7]). The mutual coherence $\kappa(\boldsymbol{A})$ is an incoherence measure that is easy to compute, $\kappa(\boldsymbol{A}) = \max_{i,j,i \neq j} |\boldsymbol{a}_i^{\text{H}} \boldsymbol{a}_j|$ where $\boldsymbol{a}_n$ is the nth normalized column of $\boldsymbol{A}$, $\|\boldsymbol{a}_n\| = 1$, $n = 1, 2, ..., N$.

In radar signal processing, a sensing matrix $\boldsymbol{A}$ is intrinsically deterministic and its incoherence is also intrinsically strong because of the physics of radar sensing. In array processing as in (1), the sensing matrix $\boldsymbol{A}$ from (2) is often taken to be an FFT matrix, i.e. $\kappa(\boldsymbol{A}) = 0$ when $M = N$. Accordingly, with a uniform array of size M, the grid cell $\Delta\theta$ is $2\pi/M$ large. Such a cell size is called the Nyquist size. Fewer measurements, i.e. when $M < N$, or a smaller cell $\Delta\theta$ would make $\kappa(\boldsymbol{A})$ increase.

III. Stochastic Resolution Analysis

Our resolution analysis is based on distances between two populations that have been studied in information geometry (IG). IG studies manifolds in the parameter space of probability distributions, using the tools of differential geometry (e.g. [5-6]). The inner product of two vectors $\boldsymbol{v}$ and $\boldsymbol{w}$ in a Euclidean space: $\langle \boldsymbol{v}, \boldsymbol{w} \rangle = \boldsymbol{v}^{\text{H}}\boldsymbol{w}$ is redefined locally as: $\langle \boldsymbol{v}, \boldsymbol{w} \rangle = \boldsymbol{v}^{\text{H}}\boldsymbol{G}\boldsymbol{w}$, where $\boldsymbol{G}$ is a crucial metric defined by the Fisher information matrix (FIM) in IG.

In an array whose measurement y_m is modeled as in (1), the FIM $G(\theta)$ for a parameter θ and a Gaussian pdf $p(\boldsymbol{y}|\theta)$ can be written as (e.g. [12] and [15]):

$$G(\theta) = -\mathrm{E}\left[\frac{\partial^2 \ln p(\boldsymbol{y}|\theta)}{\partial \theta^2}\right] = 2\text{SNR}\|\boldsymbol{\beta}\|^2 = G_\theta \,. \qquad (4)$$

In the estimation theory, the metric $G(\theta)$ is typically used to derive the Cramér-Rao bound (CRB) of the mean squared error (MSE) of an unbiased estimator $\hat{\theta}$ of θ, i.e. $\text{MSE}(\hat{\theta}) \geq \text{CRB}(\theta) = 1/G(\theta)$ (e.g. [15]). Alternatively, we explore how $G(\theta)$ can also be used to compute resolution bounds based on

information distances between $p(\boldsymbol{y}|\theta)$ and $p(\boldsymbol{y}|\theta + d\theta)$ when a parameter θ changes a bit by $d\theta$ (e.g. [4-6]).

A. Information Distances

Among many types of information distances (e.g. [6]), we start with the Fisher-Rao information distance (FRID) because it is directly related to the basic IG infinitesimal Fisher-Rao metric ds, i.e. the Riemann metric ds associated with the FIM $G(\theta)$, $ds^2 = G(\theta)d\theta^2$. Moreover, most IG (pseudo-)distances such as e.g. the Kullback-Leibler (KL) divergence and Bhattacharyya (BT) distance, reduce to simple functions of ds and the FRID, especially, in the case of Gaussian-distributed measurements.

Since we are mostly interested in θ, we parametrize the Gaussian pdf $p(\boldsymbol{y}|\theta)$ in θ first ([12]). The FRID d_θ on the 1D manifold in θ is a geodesic computed from the integrals of ds over possible curves, as:

$$d_\theta \equiv \min_{\vartheta(t)} \int_0^1 \sqrt{\left[\dot{\vartheta}(t)\right]^2 G(\vartheta(t))} \, dt \,,$$

where $\vartheta(t)$ is a coordinate of an integration path parameterized by t, $t \in [0\ 1]$. The coordinate $\vartheta(t)$ is computed from the geodesic equations (e.g. [4-6]) written as:

$$\ddot{\vartheta}(t) + C[\dot{\vartheta}(t)]^2 = 0, \qquad C = G_\theta^{-1} \partial G_\theta / \partial \theta$$

where C is a connection coefficient. For (1), C is zero as $G(\theta)$, is constant w.r.t. θ, $G(\theta) \equiv G_\theta$, i.e. $\ddot{\vartheta}(t) = 0$. Thus, the integration curve is a line given by: $\vartheta(t) = \delta\theta t + \theta$, $t \in [0\ 1]$. Accordingly, the FRID d_θ between $p(\boldsymbol{y}|\theta)$ and $p(\boldsymbol{y}|\theta + \delta\theta)$ on the 1D statistical manifold is given by ([13]):

$$d_\theta \equiv \min_{\vartheta(t)} \int_0^1 \sqrt{G_\theta[\dot{\vartheta}(t)]^2} \, dt = \sqrt{G_\theta}\,\delta\theta = \sqrt{2\text{SNR}}\,\|\boldsymbol{\beta}\|\delta\theta \,. \quad (5)$$

Note that d_θ has no unit because $\delta\theta$ is actually normalized with the corresponding Rayleigh distance $1/\|\boldsymbol{\beta}\|$.

In [13], we noticed that d_θ and its related resolution were too optimistic. This is due to the fact that the radar model function $\boldsymbol{\mu}(\theta)$ is nonlinear, while the FRID d_θ can be interpreted as the Taylor expansion of a distance function. Hence, another information distance $d_{\boldsymbol{\mu}(\theta)}$ related directly to the mean $\boldsymbol{\mu}(\theta)$ of the data $\boldsymbol{y}$ from (2) can be used. Accordingly, tighter resolution bounds are to be expected.

The information distance $d_{\boldsymbol{\mu}(\theta)}$ between $CN(\boldsymbol{\mu}(\theta), \gamma \boldsymbol{I}_M)$ and $CN(\boldsymbol{\mu}(\theta + \delta\theta), \gamma \boldsymbol{I}_M)$ with mean difference $\delta\boldsymbol{\mu}$, $\delta\boldsymbol{\mu} = \boldsymbol{\mu}(\theta + \delta\theta) - \boldsymbol{\mu}(\theta)$, but the same covariance matrix is derived analog to the distance d_μ from [5] between $N(\mu, \gamma)$ and $N(\mu + \delta\mu, \gamma)$ on the 2D manifold in $(\mu, \sqrt{\gamma})$. Accordingly, the distance $d_{\boldsymbol{\mu}(\theta)}$ is equal to the Mahalanobis distance, given by:

$$d_{\boldsymbol{\mu}(\theta)} = \sqrt{\delta\boldsymbol{\mu}^H \boldsymbol{G}_{\boldsymbol{\mu}} \delta\boldsymbol{\mu}} = \|\delta\boldsymbol{\mu}\|/\sqrt{\gamma/2} \;\neq\; d_\theta = \sqrt{G_\theta}\,\delta\theta. \quad (6)$$

where $\boldsymbol{G}_{\boldsymbol{\mu}}$ is the FIM for the mean $\boldsymbol{\mu}$, $\boldsymbol{G}_{\boldsymbol{\mu}} = 2\boldsymbol{I}_M/\gamma$. The distance $d_{\boldsymbol{\mu}(\theta)}$ in (6) is truly no FRID but an upper bound of the geodesic (e.g. [19]). The FRID can be computed numerically by using the method of geodesic shooting (e.g. [20]).

Note that $d_{\mu(\theta)} \neq d_\theta = \sqrt{G_\theta}\, \delta\theta$, and that $d_{\mu(\theta)}$ would be equal to d_θ only if $\mu(\theta)$ would be an affine transformation of θ. This is not the case in radar because radar-echo models like $\mu(\theta)$ are nonlinear in θ. Yet, recall that the IG infinitesimal metric $ds(\theta)$, $ds^2(\theta) = d\theta^2 G_\theta$, is invariant to a different parameterization, i.e. if $\mu = \mu(\theta)$, $G_\mu = d\mu^H/d\theta\, G_\mu\, d\mu/d\theta$ and $ds^2(\mu) = d\mu^H G_\mu d\mu = d\theta^2 G_\theta = ds^2(\theta)$.

Regarding links to CS, we can note that the non-zero cross-correlation between $a(\theta)$ and $a(\theta + \delta\theta)$ from the mutual coherence $\kappa(A)$ makes $d_{\mu(\theta)}$ decrease, $d_{\mu(\theta)} = \|\delta\mu\|/\sqrt{\gamma/2} = \sqrt{2\text{SNR}(1 - Re\{a^H(\theta)a(\theta + \delta\theta)\})}$, where $a(\theta)$ is a column of the sensing matrix A at θ. The sparsity in this framework is also being interpreted (as a subject of further work). In particular, the questions arise how the sparsity may benefit from $d_{\mu(\theta)}$ rather than from d_θ and how the geometry of the Laplacian manifold can be incorporated (e.g. [21]).

Next we derive the stochastic resolution bounds from the different information distances as the probability that two targets can be resolved at a separation $\delta\theta$ and a particular SNR.

B. Resolution Bounds

In some early work on IG [5], Rao proposed testing a hypothesis $H_0: \delta\theta = 0$ and its alternative $H_1: \delta\theta \neq 0$, by using a FRID between the populations $p(y|\theta)$ and $p(y|\theta + \delta\theta)$.

In [13], we tested the same hypotheses (for two targets) via the generalized likelihood ratio (GLR) given by ([22] and [3]):

$$\text{GLR} = \left. p(y|\theta, \theta + \delta\theta)/p(y|\theta) \right|_{\delta\theta = \delta\theta_{\text{ML}}}, \quad (7)$$

where $\delta\hat{\theta}_{\text{ML}}$ is the maximum likelihood (ML) estimate of $\delta\theta$. The statistic $\ln\text{GLR}$ in (7) is asymptotically χ^2-distributed with one degree of freedom, and can be written as (e.g. [22] in 6):

$$\ln\text{GLR} \xrightarrow{a} \ln a\text{GLR} = G\left(\theta + \delta\hat{\theta}_{\text{ML}}\right)\delta\hat{\theta}_{\text{ML}}^2 = G_\theta \delta\hat{\theta}_{\text{ML}}^2 \sim \chi_{\varepsilon,1}^2 \quad (8)$$

as $\delta\hat{\theta}_{\text{ML}}\sqrt{G_\theta} \sim N(\delta\theta, 1)$. In [12-13], ε is linked to d_θ by:

$$\varepsilon = G(\theta + \delta\theta)\delta\theta^2 \equiv G_\theta \delta\theta^2 \equiv d_\theta^2 \quad . \quad (9)$$

The proof can be found in [23]. Hence, in [13], we derived the probability of resolution P_{res} for two targets as follows:

$$P_{\text{res}} = \mathbb{P}\{\ln a\text{GLR} > \rho \mid H_1\}, \quad \ln a\text{GLR} \sim \chi_{\varepsilon,1}^2. \quad (10)$$

where ρ is the threshold obtained under H_0 from the inverse χ^2-distribution at a probability of false alarm P_{fa}, $\rho = \chi_{0,1}^{2,\text{inv}}(P_{\text{fa}})$.

Since the resolution bounds from (10) were too optimistic, we derive here a closer distance $d_{\mu(\theta)}$ in (6), and explore the same likelihood ratio (LR), $\text{LR} = p(y|\theta, \theta + \delta\theta)/p(y|\theta)$, at the true separation $\delta\theta$ with the equivalent hypotheses expressed as:

$$\begin{aligned} H_0 &: y = 2\mu(\theta) + z = y_0 \\ H_1 &: y = \mu(\theta) + \mu(\theta + \delta\theta) + z = y_0 + \delta\mu \end{aligned} \quad . \quad (11)$$

where the measurements y as in (1) contain responses from two point-targets separated by $\delta\theta$. Note that we can actually interpret the resolution test from (11) as a test of detecting $\delta\mu$.

From (11), we can derive a test statistic $\ln\text{LR}$ as follows:

$$\ln\text{LR} = 2Re\{[y - 2\mu(\theta)]^H \delta\mu\}/\gamma \sim N(d_{\mu(\theta)}^2, d_{\mu(\theta)}^2) \quad (12)$$

which is Gaussian distributed with mean and variance equal to $d_{\mu(\theta)}^2$, or $\ln\text{LR}/d_{\mu(\theta)} \sim N(d_{\mu(\theta)}, 1)$. Here again we have linked a resolution test statistic with (an upper bound of) a FRID. Moreover, we can test $\ln\text{LR}$ directly, and need no asymptotic $\ln\text{GLR}$. This implies a test closer to the measurements and tighter resolution bounds.

The statistic $\ln\text{LR}$ from (12), is tested against a threshold ρ_μ obtained under H_0 from the inverse normal distribution at the false-alarm probability P_{fa}, $\rho_\mu = N^{\text{inv}}(0, d_{\mu(\theta)}^2, P_{\text{fa}})$, to assess the probability of resolution $P_{\text{res},\mu}$ as follows:

$$P_{\text{res},\mu} = \mathbb{P}\{\ln\text{LR} > \rho_\mu \mid H_1\}, \quad \ln\text{LR} \sim N(d_{\mu(\theta)}^2, d_{\mu(\theta)}^2). \quad (13)$$

In addition, in cases as in (1) with Gaussian-distributed measurements y, we can extend (13) by applying other information (pseudo-)distances such as the KL divergence d_{KL} and BT distance d_{BT}, because they are directly related to $d_{\mu(\theta)}$. More specifically, d_{KL} and d_{BT} between $p(y|\theta)$ and $p(y|\theta + d\theta)$ can be easily derived as follows:

$$\begin{aligned} d_{\text{KL}} &= E_{H_1}[\ln\text{LR}] = d_{\mu(\theta)}^2 \\ d_{\text{BT}} &= -\ln E_{H_0}[\sqrt{\text{LR}}] = d_{\mu(\theta)}^2/4 \end{aligned} \quad . \quad (14)$$

Finally, the resolution bounds given by the FRID-based probabilities P_{res} and $P_{\text{res},\mu}$ are compared with the SSP resolution whose probability $P_{\text{res,SSP}}$ is assessed numerically from x_{SSP} in (3) for the two target cells i and j, $i \neq j$, by:

$$P_{\text{res,SSP}} = \mathbb{P}\{(x_{\text{SSP},i} \neq 0) \wedge (x_{\text{SSP},j} \neq 0) \mid H_1\} \quad (15)$$

where SSP in (3) uses p equal to 0 or 1 ([17]), and η related to P_{fa} as: $\eta^2 = -\gamma\ln P_{\text{fa}} \equiv \chi_{0,2}^{2,\text{inv}}(P_{\text{fa}})/2$ (e.g. [14] and [18-19]).

IV. NUMERICAL RESULTS

The stochastic resolution analysis presented in Section III is demonstrated with numerical tests from array processing with two close equal targets at different input SNRs. The measurements y from (1) are acquired from a linear array of size M, and contain responses from two point-targets separated by $\delta\theta$, $y = \mu(\theta) + \mu(\theta + \delta\theta) + z$. The estimation grid size N is kept the same. It is Nyquist if $N = M$, or not if $N > M$, with M randomly chosen. The targets are placed in the middle of the estimation grid, and are separated in θ by $\delta\theta$ equal to $2\pi/N$ or $4\pi/N$. The amplitude α_0 is nonrandom, $\alpha_0^2 = \gamma\text{SNR}$. The noise variance γ is kept constant, $\gamma = 1$. In the thresholds ρ, ρ_μ and η in (10), (13) and (15), respectively, the false-alarm probability P_{fa} is set to 0.000001 (as realistic in radar).

The FRID-based probabilities P_{res} and $P_{\text{res},\mu}$ from (10) and (13) use the true ε and $d_{\mu(\theta)}$ from (9) and (6), respectively. The probability $P_{\text{res,SSP}}$ from (15) is assessed numerically from 100

noise runs. SSP from (3) with the l_1-norm is performed with yall1 ([24]) and with the l_0-norm via an exhaustive search.

In Fig. 1, the different information (pseudo-)distances d_θ, $d_{\boldsymbol{\mu}(\theta)}$, d_{KL} and d_{BT} from (5), (6) and (14) are illustrated for the
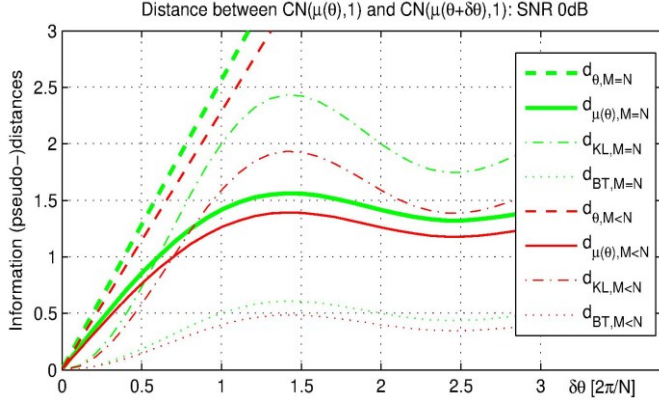

Fig. 1. Information distances from (5), (6) and (14) in test cases from (1) with two targets separated by $\delta\theta$ (expressed in Nyquist cells). Green and red indicate M equal to or smaller than N, respectively.
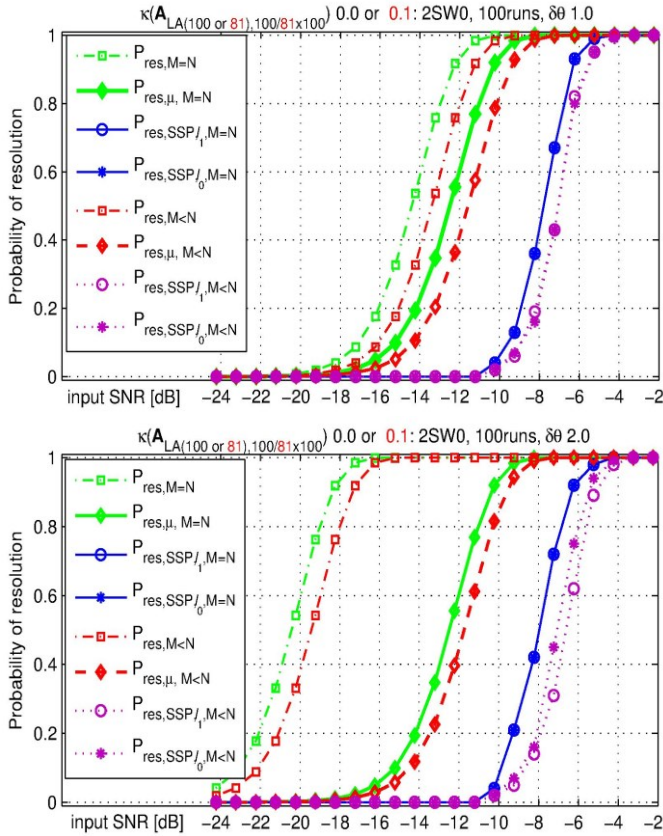

Fig. 2. Resolution bounds P_{res} and $P_{\mathrm{res},\mu}$ from (10) and (13) (squares and diamonds), respectively, compared with SSP resolution $P_{\mathrm{res,SSP}}$ from (15) (circles and stars with l_1 and l_0 norm, respectively) in a test case from (1) with two equal point-targets separated in θ by $\delta\theta$ equal to one (top) and two (bottom) Nyquist cells of an array of full size 100. Green or red in the bounds, and blue or purple in SSP, indicate the resolution with M equal to or smaller than N, respectively.

same test case from array processing. While d_θ grows linearly with $\delta\theta$, $d_{\boldsymbol{\mu}(\theta)}$ reaches its maximum quite fast (at around 1.4 Nyquist cell) and stays around that value despite the growing separation $\delta\theta$. The same tendency holds also for d_{KL} and d_{BT}. The information distances d_{KL} and d_{BT} are squared versions of $d_{\boldsymbol{\mu}(\theta)}$ as given in (14). With fewer measurements, i.e. when $M < N$, all information distances decrease.

In Fig. 2, the resolution probabilities P_{res}, $P_{\mathrm{res},\mu}$ and $P_{\mathrm{res,SSP}}$ are shown for the same test cases. The FRID-based stochastic bounds P_{res} and $P_{\mathrm{res},\mu}$ are far from $P_{\mathrm{res,SSP}}$, e.g. 6dB and 4dB at high probability 0.9 and separation 1.0 in Fig. 2, top, respectively. The SSP resolutions $P_{\mathrm{res,SSP},l_1}$ and $P_{\mathrm{res,SSP},l_0}$ are close because of low coherence $\kappa(\boldsymbol{A})$. In addition, at larger $\delta\theta$ (Fig. 2, bottom), P_{res} increases clearly while $P_{\mathrm{res},\mu}$ and $P_{\mathrm{res,SSP}}$ remain realistic, i.e. nearly the same. This behavior agrees with the related information distance $d_{\boldsymbol{\mu}(\theta)}$ in Fig. 1 that also remains nearly the same at separations $\delta\theta$ equal to 1.0 and 2.0.

V. Conclusions

A stochastic resolution analysis was presented that enables computing resolution bounds based on an information-geometry (IG) approach. The bounds are demonstrated in a typical radar application for an array configuration by a probability of resolution at a given target separation and SNR. The probability of resolution is assessed via an LR test by exploiting information distances. In particular, the Fisher-Rao information distance was recognized in the distribution of the LR. In addition, there were also other information distances from IG identified in Gaussian cases.

The resolution bounds are crucial when using fewer measurements which is typical for compressive data acquisition in the front-end of a CS sensor. In the back-end, the resolution bounds are also relevant for quantifying the SSP high-resolution performance. In array processing, this means that we consider not only the main-lobe width of the point spread function that depends on the array configuration, but also the SNR effects from fewer measurements that can be acquired by spatial or temporal sparse sensing. The SNR effects can be seen in our resolution bounds as they are based on information distances from IG that include the Fisher information. For the performance guarantees, we complete the stochastic resolution description by employing an LR test for assessing the probability of resolution at a given separation and SNR. These IG-based LR tests give significantly higher resolution bounds as compared to the SSP resolution.

This IG approach to resolution analysis enables us also to conclude that the stochastic resolution analysis is appropriate in radar (but not limited to radar) because of the sensitivity to the factors that are crucial for the resolution performance guarantees: the array configuration (or sensor design) as well as input SNR, separation and probability of resolution.

In future work, this stochastic resolution analysis based on IG is being further interpreted, and applied to multiple radar parameters in sub-Nyquist data models of CS radar. Links to the information theory are also being explored.

REFERENCES

[1] A. J. den Dekker and A. van den Bos, "Resolution: a survey", *J. of the Opt. Soc. of America A*, 14/3, 1997.

[2] S. T. Smith, "Statistical resolution limits and the complexified CR bounds", *IEEE Trans. on SP* 53/5, 2005.

[3] Zhi Liu and A. Nehorai, "Statistical angular resolution limit for point sources", *IEEE Trans. on SP* 55/11, 2007.

[4] Y. Cheng, X. Wang, T. Caelli, X. Li and B. Moran, "On information resolution of radar systems", *IEEE Trans on AES* 48/4, 2012.

[5] C. R. Rao. Information and the accuracy attainable in the estimation of statistical parameters. Bull. Calcutta Math.Soc. 37, pp. 81-89, 1945.

[6] S. Amari. "Information geometry of statistical inference - an overview", *IEEE* IT Workshop, 2002.

[7] D. Donoho, "Compressed sensing," *IEEE Trans. on IT* 52/4, 2005.

[8] E. Candès and C. Fernandez-Granda, "Towards a Mathematical Theory of Super-resolution", Willey Communications on Pure and Aplied Mathematics, vol.67/no.7, 2014.

[9] G. Schiebinger, E. Robeva and B. Recht, "Superresolution without Separation", *IEEE* CAMSAP 2015.

[10] E. de Jong and R. Pribić, "Sparse signal processing on estimation grid with constant information distance applied in radar", *EURASIP Journal on Advances in SP,* 2014:78.

[11] M. Coutino, R. Pribić and G. Leus, "Direction of arrival estimation based on information geometry", *IEEE* ICASSP 2016.

[12] R. Pribić, M. Coutino and G. Leus, "Stochastic Resolution Analysis of Co-prime Arrays in Radar", *IEEE* SSP 2016.

[13] R. Pribić, "Stochastic Resolution Analysis via a GLR Test in Radar", *IEEE* CoSeRa 2016.

[14] R. Pribić and I. Kyriakides, "Design of Sparse-signal processing in Radar Systems," *IEEE* ICASSP 2014.

[15] H. L. Van Trees. *Optimum Array Processing*. Wiley, 2002.

[16] C. E. Cook and M. Bernfeld. *Radar signals; an introduction to theory and application.* Acad.Press, 1967.

[17] R. Tibshirani, "Regression Shrinkage and Selection via the Lasso", J. of R. Stat. Soc, Series B, Vol. 58/issue 1, 1996.

[18] J.J. Fuchs, "The GLRT and the Sparse Representations Approach", vol. 6134, pp. 245–253, of *ICISP in Lecture Notes in Computer Science*. Springer Berlin Heidelberg, 2010.

[19] J. L. Strapasson, J. Pinele and S.I.R. Costa, "A Totally Geodesic Submanifold of the Multivariate Normal Distributions and Bounds for the Fisher-Rao Distance," IEEE ITW 2016.

[20] M. Pilté and F. Barbaresco, "Tracking quality monitoring based on information geometry and geodesic shooting," IRS 2016.

[21] Salem Said, Lionel Bombrun and Yannick Berthoumieu, "New Riemannian Priors on the Univariate Normal Model," Entropy, MDPI, 2014, 16, pp.4015 – 4031.

[22] S.M Kay. *Fundamentals of Statistical Signal Processing Vol. II: Detection Theory*. Prentice Hall, 1998.

[23] H. Hajri, S. Said, Y. Berthoumieu. Maximum likelihood estimators on manifolds. SEE GSI 2017.

[24] yall1: your algorithms for L1, yall1.blogs.rice.edu/.